# MOFs with Open Metal(III) Sites for the Environmental Capture of Polar Volatile Organic Compounds

Maria Inês Severino, Abeer Al Mohtar, Carla Vieira Soares, Cátia Freitas, Nicolas Sadovnik, Shyamapada Nandi, Georges Mouchaham, Vanessa Pimenta, Farid Nouar, Marco Daturi, et al.

# MOFs with Open Metal(III) Sites for the Environmental Capture of Polar Volatile Organic Compounds

Maria Inês Severino,[a,e] Abeer Al Mohtar,[b,e] Carla Vieira Soares,[c,e] Cátia Freitas,[b] Nicolas Sadovnik,[d] Shyamapada Nandi,[a] Georges Mouchaham,[a] Vanessa Pimenta,[a] Farid Nouar,[a] Marco Daturi,[d] Guillaume Maurin*,[c] Moisés L. Pinto*,[b] Christian Serre [a]*

[a] Institut des Matériaux Poreux de Paris (IMAP), ESPCI Paris, Ecole Normale Supérieure, CNRS, PSL University, 75005 Paris, France
E-mail: christian.serre@espci.psl.eu
[b] CERENA, Departamento de Engenharia Química, Instituto Superior Técnico, Universidade de Lisboa, 1049-001 Lisboa, Portugal
Email : moises.pinto@tecnico.ulisboa.pt
[c] ICGM, Univ. Montpellier, CNRS, ENSCM, Montpellier, 34293, France
Email : guillaume.maurin1@umontpellier.fr
[d] Normandie Univ., ENSICAEN, UNICAEN, CNRS, Laboratoire Catalyse et Spectrochimie, 14000 Caen, France
[e] These authors contributed equally: Maria Inês Severino, Abeer Al Mohtar, Carla Vieira Soares

Supporting information for this article is given via a link at the end of the document

**Abstract:** Metal-Organic Frameworks (MOF) with open metal sites (OMS) interact strongly with a range of polar gases/vapors. However, under ambient conditions, their selective adsorption is generally impaired due to a high OMS affinity to water. This led previously to the privilege selection of hydrophobic MOFs for the selective capture/detection of volatile organic compounds (VOCs). Herein, we show that this paradigm is challenged by metal(III) polycarboxylates MOFs, bearing a high concentration of OMS, as MIL-100(Fe), enabling the selective capture of polar VOCs even in the presence of water. With experimental and computational tools, including single-component gravimetric and dynamic mixture adsorption measurements, *in situ* infrared (IR) spectroscopy and Density Functional Theory calculations we reveal that this adsorption mechanism involves a direct coordination of the VOC on the OMS, associated with an interaction energy that exceeds that of water. Hence, MOFs with OMS are demonstrated to be of interest for air purification purposes.

## Introduction

Volatile organic compounds (VOCs) are still a major health concern, with their presence in air being documented as associated to high health risks including cancer.[1], [2] The European Community defines VOCs as any organic compound having, at 25 °C, a vapor pressure above 0.01 kPa, or a corresponding volatility under the same particular conditions.[3] Thus, these compounds can evaporate under ambient temperature and atmospheric pressure compromising air quality, consequently, increasing health risks. Therefore, stricter indoor air quality guidelines are emerging and they are currently turning into regulations in several countries around the world.[4]–[7]

The VOCs concentration in indoor environments is commonly attenuated by simple ventilation. However, this requires a high amount of energy and it is not often sufficient, notably when the sources of VOCs are present. Other complementary approaches have been envisaged, including biological treatment (bio filtration, bio-scrubbers, etc.)[8], catalytic oxidation,[9] or ionization methods (plasma, etc.)[10]. Yet, the removal of VOCs from indoor air is still a great challenge especially due to the low concentration and large diversity of vapors.[11]

Adsorption is a commonly used technique for indoor air quality improvement.[12] Various classes of porous materials have been considered to date as possible solutions such as zeolites and activated carbons.[11], [13]–[16] However, these sorbents present important limitations for the capture of polar VOCs under atmospheric conditions where the relative humidity levels impair their selective adsorption performance. This is for instance the case for acetic acid (AA), an acidic polar VOC that is associated to the degradation of cellulose and the so-called 'Vinegar Syndrome'. High performing adsorbents are indeed considered to capture traces of AA in the presence of air humidity to protect these artefacts (lead, lead alloys, copper alloys, metal surfaces, papers, cellulose-acetate-based, papers, calcareous materials, etc[17]–[23]). However, activated carbons have shown a limited AA affinity while zeolites' performance is hampered by their strong hydrophilic character, and consequently results in a low selectivity. Metal-Organic Frameworks (MOFs) have recently been proposed as potential alternatives for the capture of VOCs.[24] These highly tunable hybrids crystalline micro- or meso-porous solids exhibit several key features for the capture of VOCs such as high surface area, variable pore size/shape and hydrophilic/hydrophobic balance usually associated with mild regeneration conditions. Thus, for a given VOC capture application, ideal MOF adsorbents can be selected. In the case of AA capture, it has been shown that the microporous Zr-MOFs denoted MIL-140B(Zr) or UiO-66(Zr)-2$CF_3$, (MIL and UiO stand for Materials from Institut Lavoisier and University of Olso, respectively), due to their combination of narrow pores (≈ 4-6 Å) and hydrophobic character, associated with a moderate AA affinity, resulted in an efficient capture of this VOC in museum conditions.[24] However, these hydrophobic materials performances are still limited by the presence of (polar) defects that impair their ability to exhibit a very low water uptake at the standard humidity rate for the application, i.e., $p/p_0 < 0.45$. In general, the incorporation of open metal sites (OMS) in MOFs can increase the adsorption interactions with a wide range of polar or quadrupolar gas molecules[25]. This includes the capture of $CO_2$ (*versus* $CH_4$)[26], $N_2$[27], CO[28], [29], the separation of acidic or basic gases or vapors NO[30], [31], $N_2O$[32], $NH_3$, $SO_x$[26], [33], $H_2S$[34], the separation of olefins[35] and the trapping of other chemical harmful

agents (dimethyl methylphosphonate)[36]. Since the presence of OMS increases the interaction strength with polar molecules, the use of MOFs with active sites, particularly porous water stable metal(III) based MOFs, can also be of interest for the capture of several VOCs. This has been studied for different MOFs structures and for different vapors with MIL-101(Cr) reported as a promising adsorbent for polar acetone, methanol, and for non-polar benzene, toluene, ethylbenzene and xylenes (due to interactions with the aromatic rings).[37] Similarly MIL-100 has shown to be a good adsorbent for toluene[38] and acetone[39]. However, these materials are also known for their relatively high water affinity, with both MIL-100(Fe) and MIL-101(Cr) extensively explored for heat reallocation purposes using water as a fluid.[40]–[42] Therefore, the highly polar water molecule present in a very large excess under environmental conditions has been speculated so far to be preferentially adsorbed instead of other families of guest molecules. Indeed, the selective adsorption towards water has shown to be favorable in drug delivery, where the deprotonated ibuprofen or phosphorilated azidothimidine are strongly attached to MIL-100(Fe) or MIL-101(Cr, Fe) OMS, and slowly released and displaced from the OMS due to the phosphates present in body fluids.[43] However, as most applications operate under ambient conditions, i.e., in the presence of air moisture, a strong competitive adsorption towards water, is expected to seriously impair the selective adsorption of other species.[44]–[47] This makes the capture of polar VOCs in air still highly challenging, unlike hydrocarbons whose adsorption results mainly from π···π stacking and/or weak Van der Waals interactions[38], [48]. The only exception of polar molecules that has been shown to be preferentially adsorbed to water in the OMS was $NH_3$ in the MOF HKUST-1, resulting from an associated interaction energy exceeding the one of water by 30 kJ $mol^{-1}$. This lead, however, to the degradation of the MOF and the dissolution of $NH_3$ forming $(NH_4)_3BTC$ species.[49] One way to overcome this challenge relied on the pore functionalization with hydrophobic groups to circumvent the detrimental effect of water in MOFs bearing OMS, such as for instance grafting hydrophobic functional groups within the pores, e.g., MIL(Cr)-Z1 (or MIL-101 NDC with 2,6 naphthalene dicarboxylic acid)[50], or with the inclusion of carbonaceous composites, e.g., graphene oxide-modified HKUST-1[51]. However, such chemical tuning is associated with important drawbacks, e.g., complex additional synthesis steps, increase in cost, potential toxicity issues, and thus, are not economically/environmentally realistic. Nevertheless, we hypothesized that the preferential adsorption of polar VOCs towards OMS could occur for MOFs possessing sufficiently polarized OMS.

Here, we report a new paradigm for the selective VOC capture under moisture air conditions that consists on selecting a MOF without the need of hydrophobicity or confinement effect. The sorbent should be a MOF bearing sufficiently strong Lewis OMS to exclusively favor the adsorption of VOC over $H_2O$ as represented in Scheme 1. This strategy offers a unique opportunity to avoid the need to design complex and expensive poorly sustainable hydrophobic MOFs. This opens the way to rely on cheaper scalable benchmark MOFs for the environmental removal of polar VOCs. We have selected here, as a first representative application, the case of AA capture in a view of the conservation of artefacts that suffer alteration/decomposition. The selected material is a prototypical MOF that comprises a high concentration of metal(III) Lewis OMS (up to 3.6 mmol $g^{-1}$)[52],

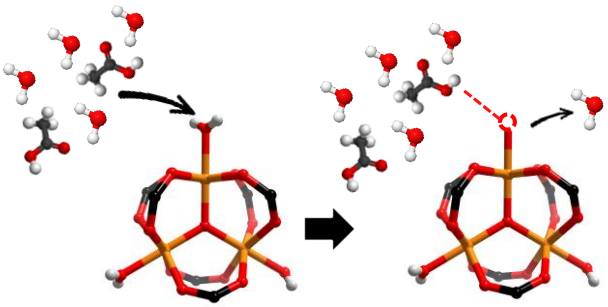

**Scheme 1.** Scheme of preferential interaction of an OMS with a highly polar vapor in a humid environment, resulting in a favorable competition with water.

e.g., MIL-100(Fe). This mesoporous iron(III) carboxylate MOF is built up from trimers of Fe(III) octahedra sharing a common vertex $\mu_3$-O and linked by the benzene-1,3,5-tricarboxylate (BTC) moieties leading to hybrid supertetrahedra[53], [54]. The latter are arranged together to generate a zeolitic architecture delimiting mesoporous cages of 25 and 29 Å, accessible through microporous windows of 5.5 and 8.6 Å, Figure 1. This MOF has been considered to date for a wide range of potential applications from storage/separation,[52], [55], [56] sensing,[57] catalysis,[58]–[61] heat reallocation,[62]–[64] to biomedical applications,[43], [65], [66] etc.

This work reports an unprecedented joint experimental/computational study that systematically explored MIL-100 platform for the selective adsorption of representative

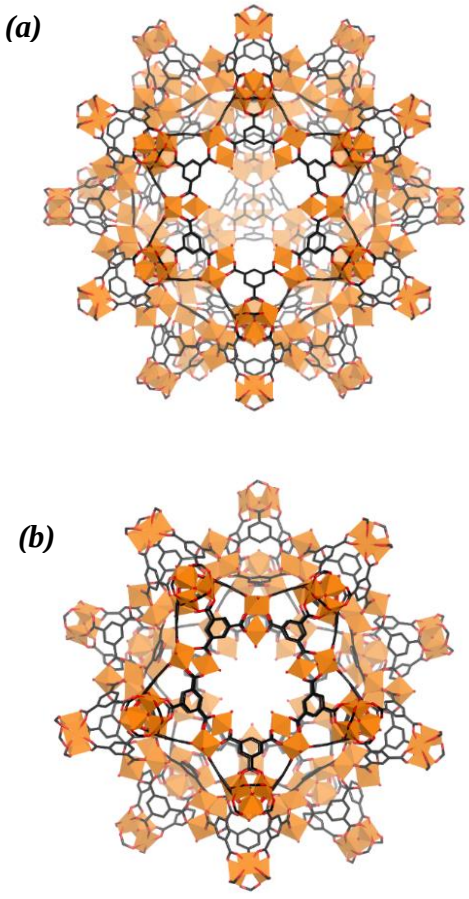


**Figure 1.** View of the small (a) and the large (b) cages of MIL-100(Fe). Iron polyhedra, carbons and oxygens are represented in orange, black and red, respectively. Hydrogen atoms are omitted for clarity.

classes of polar vapors (carboxylic acids, acetone, methanol, acetaldehyde) over water. We demonstrated that a preferential adsorption of VOCs instead of $H_2O$ on the OMS occurs for all carboxylic acids vapors whatever the nature of the metal(III) sites (Fe or Al) or the MOF structure (MIL-100, MIL-127,…). We finally illustrate the practical interest of this selective adsorption mechanism through the case of AA capture in museum conditions, paving the way for the utilization of this class of MOF in different applications, from gas chromatography detection without the need of derivatization[67]–[69], to air purification [24], [70].

## Results and Discussion

The sorption behavior of MIL-100(Fe) was first evaluated by single component gravimetric measurements for both water (see Figure 2(a)) and AA (Figure 2(b)). The synthesis of this MOF was adapted from an atmospheric pressure synthesis protocol recently reported,[62], [71] with the crystallinity confirmed and the values of the calculated BET surface area in good agreement with the previously reported data (Figure S1 to S4). MIL-100(Fe) displays a type IV water adsorption isotherm as well as a first uptake at very low partial pressures ($p/p_0$ < 0.05) associated with a full coordination of the OMS by water. This is followed by a gradual increase of the sorption uptake at intermediate relative pressures (0.20 < $p/p_0$ < 0.50) corresponding to the progressive filling of the small and large cages of the MOF[64], [72] If one compares this water adsorption behavior with other MOFs, it is seen that MIL-100(Fe) is not completely hydrophilic or hydrophobic.[24] The polar UiO-66(Zr)-$NH_2$, for instance, is much more hydrophilic, since it exhibits a steep adsorption isotherm profile at very low pressure, with one steep increase at $p/p_0$ = 0.25, while more than half the adsorption capacity is reached before $p/p_0$ = 0.3. Conversely, the more hydrophobic UiO-66(Zr)-2$CF_3$ exhibits an adsorption step that does not start before $p/p_0$ = 0.4 which is one of the reasons behind its interesting polar VOC capture ability in the presence of water.

When it turns to AA adsorption (Figure 2(b)), MIL-100(Fe) exhibits a very steep uptake at very low relative pressures ($p/p_0$ < 0.01) which drastically deviates from the behavior of UiO-66(Zr)-2$CF_3$ that shows a much lower affinity for AA. This adsorption data suggests MIL-100(Fe) as a promising VOC sorbent. To further address the impact of the presence of coordinated water towards the AA adsorption in MIL-100(Fe), a second AA sorption isotherm was collected on a room temperature vacuum activated sample and compared to the one obtained on a sample activated at 150 °C (Figure S5 (b)). From the literature, it is known that in the first case coordinated water molecules are still present within MIL-100(Fe), while after 150 °C, under vacuum activation, all the bounded water has been evacuated.[73], [74] Surprisingly, no noticeable difference in AA adsorption isotherm was observed between these two samples leading to a similar uptake at $p/p_0$ = 0.05 close to 10 mmol $g^{-1}$. The Henry constants were determined from the initial slope of the AA and water isotherms, and they are compared in Table S1. Note that despite a slight difference between the values obtained for the thermally activated and the non-thermally activated samples, these values are much higher than those of water, suggesting a selective adsorption of AA over water. To further assess the AA/water competitive adsorption, dynamic adsorption of AA in the presence of water (60 %RH) at 25 °C was carried out in the system schematized in Figure S6,

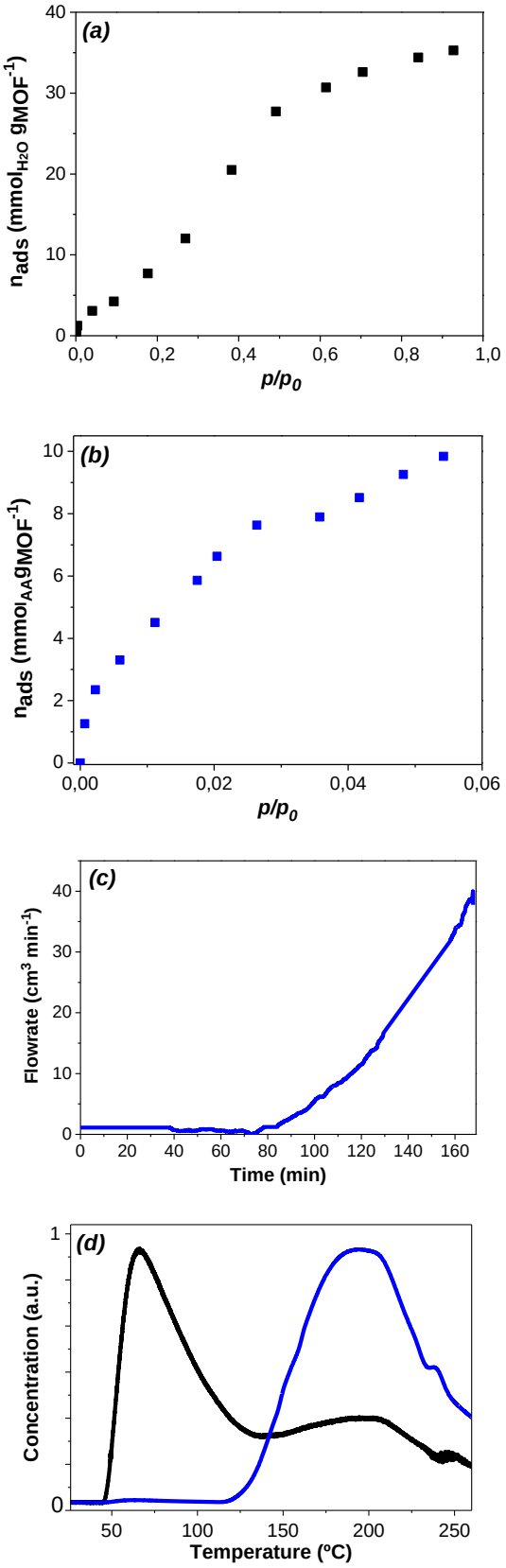


**Figure 2**. Single component (a) water adsorption and (b) AA adsorption gravimetric isotherms at 25 °C for MIL-100(Fe), (c) dynamic breakthrough profile and (d) temperature-programmed desorption of water (in black) and AA (in blue) in a 50/50 %V/V mixture on MIL-100(Fe) (Dwelling at 200 °C for 30 min).

with diluted AA concentration (500 ppm) in $N_2$ that was then carried through a packed bed of column with powder MIL-100(Fe) The column downstream was continuously monitored using a mass spectrometer. Remarkably, no AA was detected for over 80 minutes. The adsorption capacity deduced from these breakthrough tests, Figure 2 (c), seemed unchanged, with the calculated dynamic amount of the adsorbed AA (around 5.13 mmol $g^{-1}$ (Figure S7)) being comparable to the amount in equilibrium at $p/p_0 = 0.013$.

To shed light on the sorption mechanism, we first performed Temperature-Programmed Desorption (TPD) tests. TPD was adapted from the breakthrough system, where a stream of 50 % V/V of water and AA vapor was injected and carried through the bed of approximately 90 mg of the activated MIL-100(Fe) by a stream of helium. Adsorption occurred at room temperature. Then the column with the MOF was heated to trigger the desorption of the adsorbed molecules. The analyzed data was recorded and related to the temperature of the column, as it can be seen in Figure 2 (d). At around 66 °C water starts to leave the column, while AA is only visible at 196 °C, along with some extra (coordinated) water molecules that are likely to interact more strongly with the MOF structure. Thus, the desorption of AA requires much higher energy than the desorption of water, revealing a significantly stronger interaction between the OMS and AA. In addition, in the TPD of water alone, it is seen that the water starts to desorb at a slightly higher temperature (74 °C) than when the mixture is considered (Figure S10). This suggests that AA replaces water on the strongest OMS. It is of note that, this study focused on the low concentration region, since the injected amount of AA (5 µL) diluted in the helium stream corresponds to 0.0874 mmol, i.e., the maximum amount of AA that the MOF can adsorb in these conditions would be ~0.971 mmol $g^{-1}$ of MOF. Looking at the AA isotherm (Figure 2 (b)), this adsorbed amount in equilibrium lies in the Henry region, since $p/p_0 > 0.001$. Thus, the adsorption mechanism is undoubtedly governed by strong energetic interactions, presumably as a result of the high Lewis acidity of the OMS.

To get in depth understanding of the interactions of AA with the OMS, *in situ* Fourier transform infrared (FTIR) spectra were recorded for a non-activated MIL-100(Fe) sample exposed to AA (Figure 3 (a)). This revealed that AA is bonded to Lewis acid sites through the oxygen lone-pair electrons of the carbonyl group, as evidenced by the appearance of an intense ν(C=O) mode at 1690 $cm^{-1}$ (red shifted of about 92 $cm^{-1}$ in comparison to the gaseous AA) upon adsorption, regardless of activation conditions. Therefore, the presence or not of pre-coordinated water on the OMS does not impact the interactions with AA, confirming the very high selectivity of the OMS for AA adsorption *versus* water. Furthermore, adsorption of AA on non-thermally activated MIL-100(Fe) (Figure 3 (a)) revealed a progressive decrease of ν(O-H) bands at 3700-3680 and 3608 $cm^{-1}$ together with the appearance of a broad band at 3390 $cm^{-1}$, indicating the formation of hydrogen bonding between Brønsted acid sites and AA. It is worth mentioning that bands characteristic of hydrogen bonding species at around 3390 $cm^{-1}$ are also visible in the case of adsorption of AA on thermally activated MIL-100(Fe). This suggests a hydrogen bond formation between the hydroxyl group of AA and the framework.

Interestingly, upon adsorption of AA on activated sample (Figure 3 (b)), a progressive increase of bands at 3700-3680 and 3608

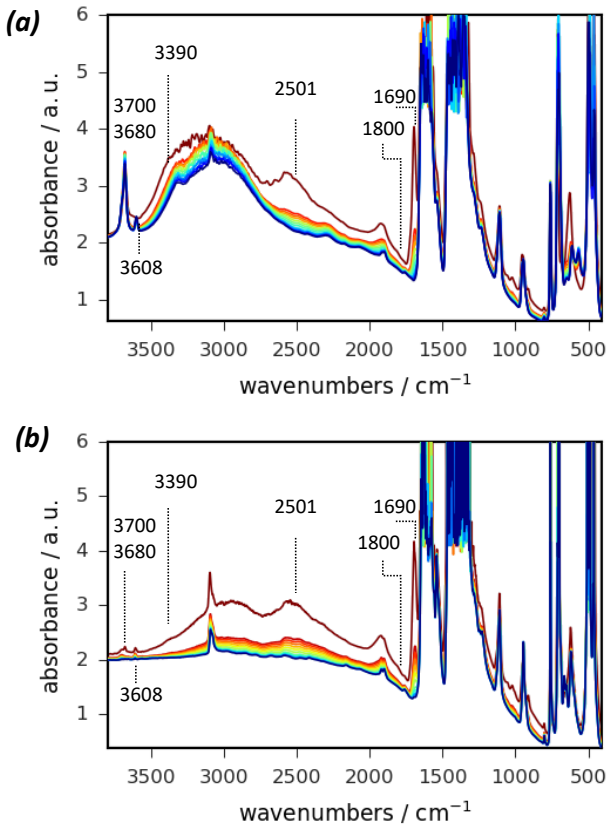


**Figure 3**. IR absorption spectra of MIL-100(Fe) recorded at 25 °C after exposure of the sample to AA a) without any thermal treatment and b) after thermal treatment at 250 °C. (From blue to red, increased doses of AA).

$cm^{-1}$ was detected which suggests a progressive restitution of Brønsted acid sites due to a partial dissociative adsorption of AA, in addition to the coordination of the molecule. In general, the weak band at about 1800 $cm^{-1}$ (ν(C=O)), in the range of gaseous AA, implies its physisorption in minor amounts.

To gain microscopic insight into the adsorption mechanism of VOCs in MIL-100(Fe), Density Functional Theory (DFT) calculations were carried out to first assess the interaction energy between the AA and a representative iron oxo-trimer cluster of the MIL-100(Fe) inorganic node (Figure S8). Figure 4 a) shows the most stable configuration of AA where its carbonyl function coordinates towards the Fe site in conjunction with the formation of a hydrogen bond between its hydroxyl group and the oxygen atom linked to the metal center, in line with the FTIR observations. Remarkably, the resulting interaction energy (-130.5 kJ $mol^{-1}$) is by far much higher than the value obtained for water coordinating on iron (-74.6 kJ $mol^{-1}$) (Figure S8). This explains the highly preferential adsorption of AA *versus* $H_2O$ towards MIL-100(Fe), as observed by dual binary adsorption experiments and evidenced by TPD. Our calculations further revealed that even when water molecules are still present on the iron site, a scenario

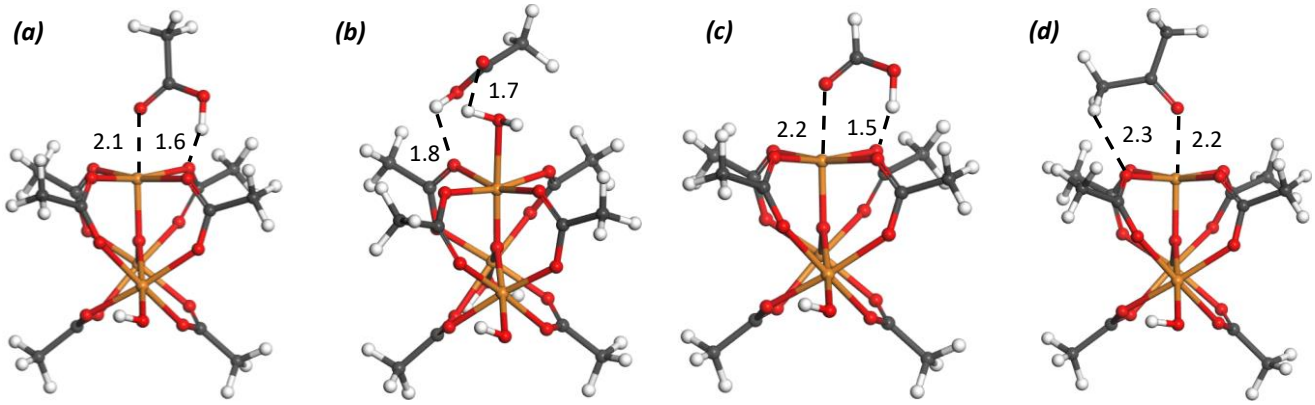


**Figure 4.** DFT-simulated most preferential geometries of (a) AA, (b) AA in the presence of water, (c) formic acid and (d) acetone, adsorbed in the MIL-100(Fe) cluster model. The interacting distances are reported in Å. Color code: Fe, orange; C, grey; O, red, H white.

encountered for the non-activated material, AA establishes strong interactions with the inorganic cluster throughout both its carbonyl function and hydroxyl groups with the coordinated water and the oxygen atom of the carboxylate respectively (Figure 4 (b), leading to high interaction energy of -99.3 kJ mol$^{-1}$, in line with the experimental observations discussed above.

To better understand the possible $H_2O$/AA exchange mechanism, climbing-image nudged elastic band (Cl-NEB) calculations were further carried out (f in SI). Figure 5 reports the corresponding minimum energy path (MEP) and the geometries of the transition states as well as the product. The initial stage corresponds to the conformation of AA in the presence of water reported in Figure 4 (b). The reaction proceeds in such a way that AA approaches the OMS Fe while the water moves away (Figure 5) and finally binds the OMS via its carbonyl group in the final state. The resulting energy barrier is moderate (47.2 kJ mol$^{-1}$), supporting the easy replacement of the coordinated water by AA as suggested experimentally. Furthermore, the similar energy between the final state and the reactant evidences the strong interactions (presence of hydrogen bonds) between AA and the MIL-100(Fe) even when water molecules are coordinated to the iron site.

DFT calculations further revealed that formic acid exhibits the same binding mode as AA (Figure 4 (c)) leading only to a slight lower interaction energy of -125.0 kJ mol$^{-1}$ as compared to AA, while it is much higher than for acetone (-88.2 kJ mol$^{-1}$) since in this last case weaker Van der Waals interactions between the alkyl group with the oxygen of the oxo-trimer cluster occur (Figure 4 (d)). Conversely, the simulated high interaction energy values for both AA and formic acid strongly suggest that these carboxylic acids preferentially adsorbed over ketones and water. This prediction encouraged us to deploy a systematic experimental study combining single component isotherms and TPD analysis for a wide range of polar vapors (Figure S11 to S14), including other carboxylic acids as well as carbonyl-based VOCs and methanol. As previously done with AA, by comparing the TPD mass spectrometer profile of the desorbed output at different temperatures, the different affinities of the molecules could be compared. In all cases, the first water peak was visible between 60 °C and 100 °C and was constantly present even at 200 °C but in a lower amount. As previously observed, for carboxylic acids the results showed a much stronger interaction with the metal centers (Figure S13). On the other hand, for carbonyl-based VOCs studied, acetone and aldehyde, the peaks appeared at lower temperatures indicating a significantly lower affinity than AA. Acetone was indeed not as strongly bound as acids, in line with the DFT predictions, with a peak appearing at ~70 °C, almost simultaneously as that of water (Figure 6 (a)). In addition, the peak of water appeared again at lower temperatures than in the TPD for water alone, suggesting still some replacement of

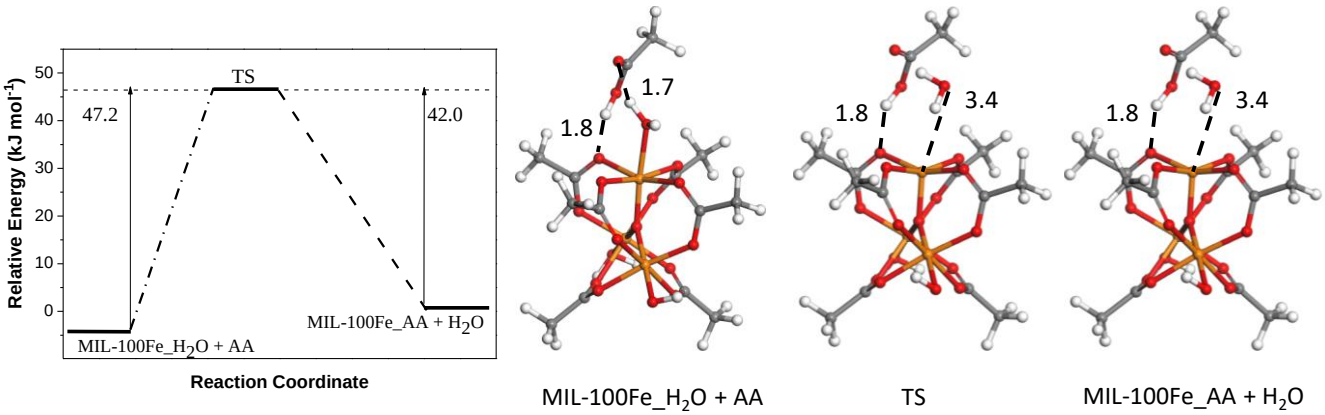


**Figure 5.** Illustration of the exchange mechanism of coordinated water by AA elucidated by Cl-NEB DFT calculations. The simulated minimum energy path and the snapshots for the reactant (MIL-100(Fe)_$H_2O$ + AA), transition state (TS) and final state (MIL-100(Fe)_AA + $H_2O$) are provided. The interacting distances are reported in Å.

adsorbed water molecules by the acetone molecules. Nevertheless, some water molecules were still more strongly bound, leaving the adsorbent at 200 °C. For the TPD with

acetaldehyde and water mixture (Figure 6 (b)), a preferential interaction with water was seen, with the last leaving 10 °C, later than acetaldehyde. However, the affinity of both molecules was quite similar, with water and acetaldehyde leaving almost simultaneous between 30 °C and 75 °C. Again, the first water peak was displaced when comparing with water in the single component TPD. Thus, the lack of additional –OH interactions resulted in less favorable interactions than for water and AA. By further comparing acetaldehyde and acetone, the slight difference in affinity can be attributed to the additional methyl group of acetone, which contributes to extra Van der Waals forces increasing the interactions with the acid sites.

Similarly, when analyzing the impact of the alkyl group of carboxylic acids, as indicated by the DFT calculations performed on formic acid, and confirmed experimentally by single component isotherm (Figure S14) and TPD spectra analysis (Figure S 12), it appeared that all carboxylic acids interact strongly with the metal centers, and the peak of this family of VOCs (e.g., for propionic acid) occurs after 150 °C, only with slight differences observed as a result of a higher energetic barrier.

For methanol the desorption was surprisingly observed at as high temperatures (T > 150 °C) as for the carboxylic acids, thus suggesting a preferred adsorption. In this case, the strong interaction can be attributed to the dissociative adsorption that leads to the formation of methoxy groups that coordinate with the iron site, as indicated by the typical methoxy bands observed on FTIR spectrum in the 3000-2800 and 1100-1000 $cm^{-1}$ regions (Figure S15).[75], [76]

With the different vapors tested, an overall sequence of interaction strength could finally be established for MIL-100(Fe) with R–COOH **>** R'–COH **>** R–CO–R' **>** R–CHO **~** $H_2O$. This sequence is in good agreement with the one obtained in the literature for other MOFs with OMS. However, this previous sequence was established in dry environment only, while the new one, performed in real conditions (humidity), confirms the limited impact of water on the adsorption of the highly polar VOCs when dealing with MOFs and metal(III) Lewis acid sites.[68], [69]

The adsorption behavior of MIL-100(Fe) was finally exploited for the removal of traces of AA in view of cultural heritage preservation, using a set-up adapted from the one previously reported by Dedecker et al.[24] This environmental chamber allows the comparison of the AA removal efficiency of MOFs in a closed controlled humid environment, that can simulate environments in museums archives. Remarkably, the activated MIL-100(Fe) achieves a substantial drop of the AA concentration from ~ 200 µg $dm^{-3}$ (injected dose) down to 30.8 µg $dm^{-3}$, after two hours of experiments (Figure 7 (a)). This result is similar to that of hydrophobic MOFs previously considered for AA capture in atmospheric conditions by Dedecker et al.[24], i.e., UiO-66(Zr)-$2CF_3$ and MIL-140B. MIL-100(Fe) is therefore an appealing candidate to substitute these hydrophobic materials for the capture of polar VOCs, particularly carboxylic acids, as, in contrasts to these solids, it can be made under green conditions based on cheap metal cations and ligands and does not suffer from defects that hamper the AA capture efficiency.

Finally, to demonstrate the versatility of this mechanism, a series of known MOFs bearing trimers of metal(III) octahedra were also explored to confirm the key role of the OMS for the removal of polar VOCs. This was the case for the microporous MIL-127(Fe) (or soc-MOF(Fe)) with about 2.7 mmol/g of OMS,[74] whose cubic structure is built up from iron(III) octahedra trimers and

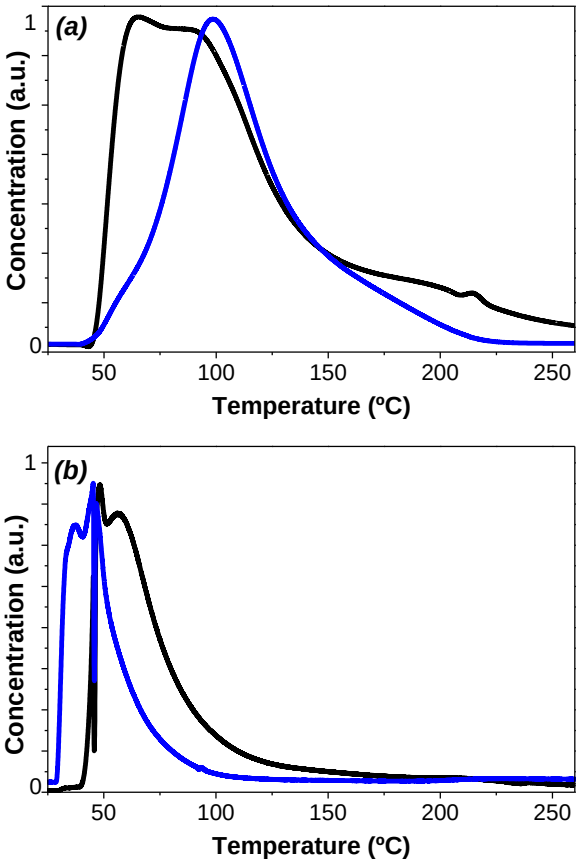


**Figure 2.** TPD spectra of organic vapors (a) acetone and (b) acetaldehyde, signalized in blue, in 50 %V/V mixture with water, signalized in black, on MIL-100(Fe) (Dwelling at 200 °C for 30 min).

tetracarboxylate ligands (TazBz), leading to two types of micropores: namely an accessible 1D channel system (~6 Å) and cages of ca. 10 Å, accessible through very narrow apertures of ~3 Å. The cages exhibit a moderate hydrophilic character due to the presence of coordinated water molecules pointing to the center of the pores, while the 1D channels exhibit a more hydrophobic character. This MOF was produced here through a previous green scalable synthesis protocol,[77] with the purity being confirmed by PXRD and nitrogen porosimetry (Figure S19 and Figure S21, respectively). Remarkably, this MOF exhibited a steep AA uptake in the single component adsorption isotherm, similar to the one of MIL-100(Fe) (Figure 7 (b)), and led under environmental chamber test to a decrease of AA concentration down to 24.5 µg $dm^{-3}$, once again similar to the performances of MIL-100(Fe), highlighting the main role of these metal(III) OMS over the selective capture of AA. It is of note that the results in the closed humid chamber gives only an initial comparison, it is in no way quantitative and as such the small deviations in the final concentration cannot be analyzed in depth.

MIL-100(Al) and MIL-101(Cr) were then tested to study the impact of the nature and concentration of OMS. The synthesis of these materials were performed following known protocols, i.e., a microwave assisted hydrothermal synthesis.[78], [79] Their crystallinity and purity were confirmed by PXRD analysis. Their calculated BET area are similar to the reported ones (Figure S22 and S23 for MIL-100(Al) and Figure S24 and S25 for MIL-101(Cr)).[78], [79] A similar behavior was observed for MIL-100(Al)

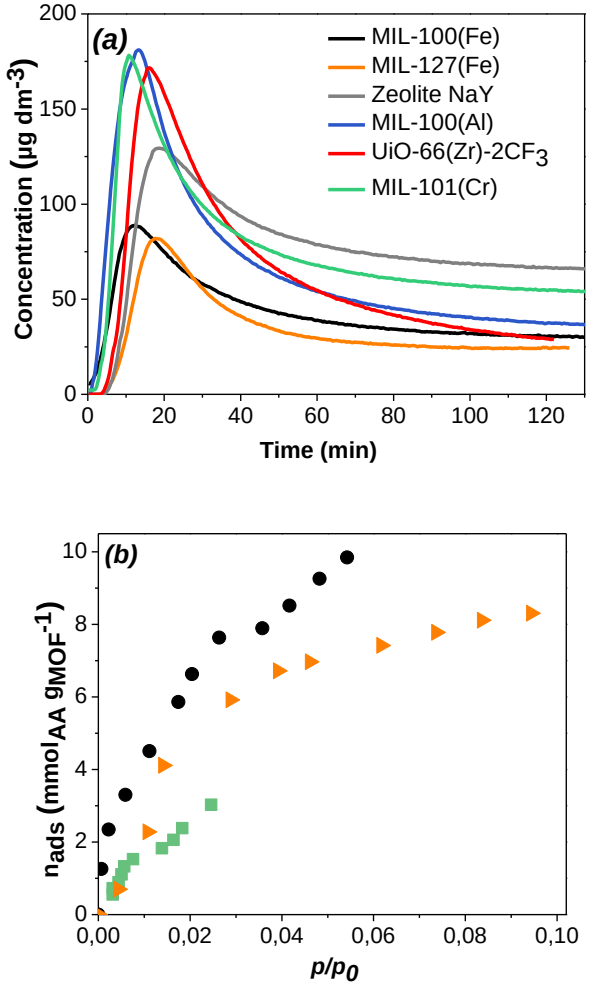


**Figure 3.** (a) AA concentration profiles of different trimer-based MOFs inside a closed chamber at 25 °C and 40 %R.H. compared with benchmark adsorbent zeolite NaY (1 µL of AA is injected equivalent to an initial concentration of 145 ppm); (b) AA single component adsorption isotherms at 25 °C of trimer-based MOFs (●) MIL-100(Fe), (▶) MIL-127(Fe) and (■) MIL-101(Cr).

in comparison with the two aforementioned Fe-MOFs already investigated, here in agreement with the presence of OMS previously reported for MIL-100(Al) (2.2 mmol $g^{-1}$ of OMS[80]), leading to a final concentration of AA in the environmental chamber of 36.6 µg $dm^{-3}$ (after two hours of exposure). On the other hand, as a counter example, we considered MIL-101(Cr), a mesoporous Cr terephthalate with Cr trimers; this MOF has been shown to exhibit not only a lower concentration of Lewis acid sites (< 1mmol $g^{-1}$) but also a lower relative strength in comparison with the MIL-100's series as a consequence of a poisoning of the strongest sites, probably by free carboxylic linkers. It was indeed already reported that the strength of Lewis acidity of MIL-100 exceeded by far the one of MIL-101(Cr).[80] Even if MIL-101(Cr) still exhibit a steep AA adsorption isotherm profile, the amount of adsorbed AA reaches only 1.5 mmol $g^{-1}$ at low relative pressures ($p/p_0$<0,01 at 25°C). As a consequence, this MOF is much less efficient to capture traces of AA under air moisture with almost 60 µg $dm^{-3}$ of AA still present in the chamber after two hours. Therefore, to achieve an efficient capture of traces of AA in a humid environment (40 %R.H.) a MOF is required to possess a minimal concentration of active metal(III) sites, i.e., typically exceeding 2 mmol $g^{-1}$. In addition, the higher hydrophobic character of MIL-101(Cr) (half the water sorption capacity being reached after $p/p_0$ = 0.5) did not seem to improve, as expected, the adsorption of AA resulting in a performance comparable to the one of the benchmark zeolite NaY commonly used for the adsorption of AA in museums showcases. Unlike the metal(III) MOFs bearing OMS, the adsorption sites of water and AA are, for cationic zeolites, similar, which is associated with an unfavorable competition between AA and water, while the highlighted MOFs adsorb AA quasi exclusively on the OMS, leaving the rest of the porosity available to adsorb free water.

## Conclusion

The capture of polar VOCs under environmental conditions, i.e., in the presence of humidity, previously relied on hydrophobic microporous sorbents. Polar carboxylate MOFs bearing Lewis acid OMS were in parallel considered as being excellent candidates for the capture of polar gases or vapors, but under dry conditions. We show for the first time, through a systematic combination of advanced experimental and computational techniques, that selected micro or meso-porous MOFs constructed from trimers of metal(III) octahedra bearing OMS, when in sufficient strength and concentration, whatever their hydrophobic character or pore size, are able to capture selectively traces of polar VOCs such as carboxylic acids in the presence of air moisture. This is due to a highly favorable sorption driven by a direct coordination of the -C=O bond on the OMS, as well as, additional hydrogen bonds between the -OH group of the carboxylic acid and the neighboring oxygens of the trimer. A classification of interactions of model polar vapors could also be determined with acids being more adsorbed than alcohols and ketones. As these MOFs are in most cases prepared under green scalable conditions based on non-expensive raw materials, this paves the way for their practical use in air purification systems or beyond for the controlled release of cosmetics or active substances.

## Acknowledgements

This work has received funding from the European Union's Horizon 2020 research and innovation programme under grant agreement No 760801 \NEMOSINE. Fundação para a Ciência e a Tecnologia (FCT-MCTES) is acknowledged for the funding to the Project UIDB/04028/2020, UIDP/04028/2020 (CERENA). This work was granted access to the HPC resources of CINES under the allocation A0120907613 made by GENCI.

**Keywords:** MOFs • Volatile Organic Compounds • Adsorption • Open Metal Sites • Acetic Acid

[1] J. Chen, Y. Huang, G. Li, T. An, Y. Hu, and Y. Li, *J. Hazard. Mater.*, **2016**, *vol. 302*, no. 302, pp. 395–403.

[2] J. E. Colman Lerner, E. Y. Sanchez, J. E. Sambeth, and A. A. Porta, *Atmos. Environ.*, **2012**, *vol. 55*, no. 55, pp. 440–447.

[3] "Proposal for a Council Directive on limitation of emissions of volatile organic compounds due to the use of organic solvents in certain industrial activities," **1996**, .

[4] C. Schlitt, P. Carrer, M. Maroni, M. Jantunen, C. Cochet, S. Kirchner, T. Lindvall, J. Mclaughlin, and L. Mølhave, “The INDEX project - Critical Appraisal of the Setting and Implementation of Indoor Exposure Limits in the EU,” **2005**.

[5] World Health Organization Regional Office for Europe, “Air Quality Guidelines for Europe,” **2006**.

[6] “Décret n° 2011-1727 du 2 décembre 2011 relatif aux valeurs-guides pour l’air intérieur pour le formaldéhyde et le benzène,” *République Française Journal Officiel Lois et Décrets*, *vol. 281*. pp. 1–437, **2011**.

[7] S. Dimitrulopoulou, C. Shrubsole, K. Foxall, B. Gadeberg, and A. Doutsi, “Indoor Air Quality Guidelines for selected Volatile Organic Compounds ( VOCs ) in the UK About Public Health England,” *UK Indoor Air Quality Guidelines for selected VOCs*. pp. 1–9, **2019**.

[8] S. Mudliar, B. Giri, K. Padoley, D. Satpute, R. Dixit, P. Bhatt, R. Pandey, A. Juwarkar, and A. Vaidya, *J. Environ. Manage.*, **2010**, *vol. 91*, no. 5, pp. 1039–1054.

[9] M. S. Kamal, S. A. Razzak, and M. M. Hossain, *Atmos. Environ.*, **2016**, *vol. 140*, pp. 117–134.

[10] P. Mohammadi, F. Ghorbani-shahna, A. Bahrami, A. A. Rafati, and M. Farhadian, *J. Photochem. Photobiol. A Chem.*, **2020**, *vol. 394*, no. 112460.

[11] E. Kabir and K. H. Kim, *Asian J. Atmos. Environ.*, **2012**, *vol. 6*, no. 3, pp. 137–146.

[12] A. Luengas, A. Barona, C. Hort, G. Gallastegui, V. Platel, and A. Elias, *Rev. Environ. Sci. Biotechnol.*, **2015**, *vol. 14*, no. 3, pp. 499–522.

[13] A. J. Cruz, J. Pires, A. P. Carvalho, and M. B. De Carvalho, *J. Chem. Eng. Data*, **2004**, *vol. 49*, no. 3, pp. 725–731.

[14] C. W. Kwong, C. Y. H. Chao, K. S. Hui, and M. P. Wan, *Atmos. Environ.*, **2008**, *vol. 42*, no. 10, pp. 2300–2311.

[15] F. Shiraishi, S. Yamaguchi, and Y. Ohbuchi, *Chem. Eng. Sci.*, **2003**, *vol. 58*, no. 3–6, pp. 929–934.

[16] F. Shiraishi and T. Ishimatsu, *Chem. Eng. Sci.*, **2009**, *vol. 64*, no. 10, pp. 2466–2472.

[17] A. W. Brokerhof and M. Van Bommel, *Deterioration of calcareous materials by acetic acid vapour: a model study*. London: James & James (Science Publishers) Ltd., 1996.

[18] L. T. Gibson and C. M. Watt, *Corros. Sci.*, **2010**, *vol. 52*, no. 1, pp. 172–178.

[19] A. L. Dupont and J. Tétreault, *Stud. Conserv.*, **2000**, *vol. 45*, no. 3, pp. 201–210.

[20] S. H. Smedemark, M. Ryhl-Svendsen, and J. Toftum, *Stud. Conserv.*, **2020**, *vol. 65*, no. 5, pp. 251–261.

[21] S. Msallamova, M. Kouril, K. C. Strachotova, J. Stoulil, K. Popova, P. Dvorakova, and M. Lhotka, *Herit. Sci.*, **2019**, *vol. 7*, no. 76, pp. 1–9.

[22] A. Al Mohtar, S. Nunes, J. Silva, A. M. Ramos, J. Lopes, and M. L. Pinto, *ACS Omega*, **Mar. 2021**, *vol. 6*, no. 12, pp. 8028–8037.

[23] A. J. Cruz, J. Pires, A. P. Carvalho, and M. Brotas de Carvalho, *J. Cult. Herit.*, **2008**, *vol. 9*, no. 3, pp. 244–252.

[24] K. Dedecker, R. S. Pillai, F. Nouar, J. Pires, N. Steunou, E. Dumas, G. Maurin, C. Serre, and M. L. Pinto, *Appl. Mater. Interfaces*, **2018**, *vol. 10*, no. 16, pp. 13886–13894.

[25] J. N. Joshi, G. Zhu, J. J. Lee, E. A. Carter, C. W. Jones, R. P. Lively, and K. S. Walton, **2018**, *vol. 34*, pp. 8443–8450.

[26] D. Britt, H. Furukawa, B. Wang, T. G. Glover, and O. M. Yaghi, *Proc. Natl. Acad. Sci. U. S. A.*, **2009**, *vol. 106*, no. 49, pp. 20637–20640.

[27] D. Liu, H. Wu, S. Wang, Z. Xie, J. Li, and W. Lin, *Chem. Sci.*, **2012**, *vol. 3*, no. 10, pp. 3032–3037.

[28] J. R. Karra and K. S. Walton, **2008**, *vol. 24*, no. 16, pp. 8620–8626.

[29] S. Chavan, J. G. Vitillo, E. Groppo, F. Bonino, C. Lamberti, P. D. C. Dietzel, and S. Bordiga, *J. Phys. Chem. C*, **2009**, *vol. 113*, no. 8, pp. 3292–3299.

[30] B. Xiao *et al.*, *J. Am. Chem. Soc.*, **2007**, *vol. 129*, no. 5, pp. 1203–1209.

[31] R. V. Pinto *et al.*, *Angew. Chemie - Int. Ed.*, **2020**, *vol. 59*, no. 13, pp. 5135–5143.

[32] J. Yang, B. Du, J. Liu, R. Krishna, F. Zhang, W. Zhou, Y. Wang, J. Li, and B. Chen, *Chem. Commun.*, **2018**, *vol. 54*, no. 100, pp. 14061–14064.

[33] T. Grant Glover, G. W. Peterson, B. J. Schindler, D. Britt, and O. Yaghi, *Chem. Eng. Sci.*, **2011**, *vol. 66*, no. 2, pp. 163–170.

[34] L. Hamon, C. Serre, T. Devic, T. Loiseau, F. Millange, G. Férey, and G. De Weireld, *J. Am. Chem. Soc.*, **2009**, *vol. 131*, no. 25, pp. 8775–8777.

[35] C. Y. Chuah, H. Lee, and T. H. Bae, *Chem. Eng. J.*, **2022**, *vol. 430*, no. 132654.

[36] F. J. Ma, S. Liu, C. Sun, G. Ren, F. Wei, Y. Chen, and Z. Su, *J. Am. Chem. Soc.*, **2011**, *vol. 133*, pp. 4178–4181.

[37] K. Yang, Q. Sun, F. Xue, and D. Lin, *J. Hazard. Mater.*, **2011**, *vol. 195*, pp. 124–131.

[38] X. Ma, W. Wang, C. Sun, H. Li, J. Sun, and X. Liu, *Sci. Total Environ.*, **2021**, *vol. 793*, no. 17923, p. 148622.

[39] X. Xie, J. Thomas, C. T. Chang, and H. Tao, *Am. Sci. Publ.*, **2021**, *vol. 21*, no. 11, pp. 5510–5521.

[40] S. Cui *et al.*, *Appl. Therm. Eng.*, **2019**, *vol. 161*, p. 114135.

[41] H. Zhao, Q. Li, Z. Wang, T. Wu, and M. Zhang, *Microporous Mesoporous Mater.*, **2020**, *vol. 297*, no. January, p. 110044.

[42] J. Ehrenmann, S. K. Henninger, and C. Janiak, *Eur. J. Inorg. Chem.*, **2011**, no. 4, pp. 471–474.

[43] P. Horcajada, R. Gref, T. Baati, P. K. Allan, G. Maurin, P. Couvreur, G. Férey, R. E. Morris, and C. Serre, *Chem. Rev.*, **2012**, *vol. 112*, no. 2, pp. 1232–1268.

[44] M. Bahri, F. Haghighat, H. Kazemian, and S. Rohani, *Chem. Eng. J.*, **2017**, *vol. 313*, pp. 711–723.

[45] K. Vellingiri, J. E. Szulejko, P. Kumar, E. E. Kwon, K. Kim, A. Deep, D. W. Boukhvalov, and R. J. C. Brown, *Nat. Publ. Gr.*, **2016**, no. April, pp. 1–11.

[46] C. Schlüsener, D. N. Jordan, M. Xhinovci, T. J. Matemb Ma Ntep, A. Schmitz, B. Giesen, and C. Janiak, *Dalt. Trans.*, **2020**, *vol. 49*, pp. 7373–7383.

[47] C. Montoro, E. Q. Procopio, I. Senkovska, S. Kaskel, S. Galli, N. Masciocchi, E. Barea, and J. A. R. Navarro, *J. Am. Chem. Soc.*, **2011**, no. 133, pp. 11888–11891.

[48] Z. Zhao, S. Wang, Y. Yang, X. Li, J. Li, and Z. Li, *Chem. Eng. J.*, **2015**, *vol. 259*, pp. 79–89.

[49] G. W. Peterson, G. W. Wagner, A. Balboa, J. Mahle, T.

Sewell, and C. J. Karwacki, *J. Phys. Chem. C*, **2009**, *vol. 113*, pp. 13906–13917.
[50] M. Zhu, P. Hu, Z. Tong, Z. Zhao, and Z. Zhao, *Chem. Eng. J.*, **2017**, *vol. 313*, pp. 1122–1131.
[51] N. Bhoria, G. Basina, J. Pokhrel, K. S. Kumar Reddy, S. Anastasiou, V. V. Balasubramanian, Y. F. AlWahedi, and G. N. Karanikolos, *J. Hazard. Mater.*, **2020**, *vol. 394*, no. 122565.
[52] J. W. Yoon *et al.*, *Angew. Chemie - Int. Ed.*, **2010**, *vol. 49*, no. 34, pp. 5949–5952.
[53] P. Horcajada, S. Surblé, C. Serre, D. Y. Hong, Y. K. Seo, J. S. Chang, J. M. Grenèche, I. Margiolaki, and G. Férey, *Chem. Commun.*, **2007**, *vol. 100*, no. 27, pp. 2820–2822.
[54] G. Férey, C. Serre, C. Mellot-Draznieks, F. Millange, S. Surblé, J. Dutour, and I. Margiolaki, *Angew. Chemie - Int. Ed.*, **2004**, *vol. 43*, no. 46, pp. 6296–6301.
[55] M. Latroche, S. Surblé, C. Serre, C. Mellot-Draznieks, P. L. Llewellyn, J.-H. Lee, J.-S. Chang, S. H. Jhung, and G. Férey, *Angew. Chemie - Int. Ed.*, **2006**, *vol. 118*, no. 48, pp. 8407–8411.
[56] S. Wuttke, P. Bazin, A. Vimont, C. Serre, Y. K. Seo, Y. K. Hwang, J. S. Chang, G. Férey, and M. Daturi, *Chem. - A Eur. J.*, **2012**, *vol. 18*, no. 38, pp. 11959–11967.
[57] J. H. Fu, Z. Zhong, D. Xie, Y. J. Guo, D. X. Kong, Z. X. Zhao, Z. X. Zhao, and M. Li, *Angew. Chemie - Int. Ed.*, **2020**, *vol. 59*, no. 46, pp. 20489–20498.
[58] M. Giménez-Marqués, A. Santiago-Portillo, S. Navalón, M. Álvaro, V. Briois, F. Nouar, H. Garcia, and C. Serre, *J. Mater. Chem. A*, **2019**, *vol. 7*, no. 35, pp. 20285–20292.
[59] N. M. Mahmoodi, J. Abdi, M. Oveisi, M. Alinia Asli, and M. Vossoughi, *Mater. Res. Bull.*, **2018**, *vol. 100*, pp. 357–366.
[60] J. N. Hall and P. Bollini, *ACS Catal.*, **2020**, *vol. 10*, no. 6, pp. 3750–3763.
[61] A. Dhakshinamoorthy *et al.*, *ACS Catal.*, **2012**, *vol. 2*, no. 10, pp. 2060–2065.
[62] S. Cui, M. Qin, A. Marandi, V. Steggles, S. Wang, X. Feng, F. Nouar, and C. Serre, *Sci. Rep.*, **2018**, *vol. 8*, no. 1, pp. 2–10.
[63] P. Hou, K. Zu, M. Qin, and S. Cui, *Build. Environ.*, **2021**, *vol. 187*, p. 107396.
[64] F. Jeremias, A. Khutia, S. K. Henninger, and C. Janiak, *J. Mater. Chem.*, **2012**, *vol. 22*, no. 20, pp. 10148–10151.
[65] X. Ma, M. Lepoitevin, and C. Serre, *Mater. Chem. Front.*, **2021**, *vol. 5*, no. 15, pp. 5573–5594.
[66] C. R. Quijia, C. Lima, C. Silva, R. C. Alves, R. Frem, and M. Chorilli, *J. Drug Deliv. Sci. Technol.*, **2021**, *vol. 61*, p. 102217.
[67] R. M. Flores and P. V. Doskey, *J. Chromatogr. A*, **2015**, *vol. 1418*, pp. 1–11.
[68] D. Zheng, Y. Zhang, L. Wang, M. Kurmoo, and M. Zeng, **2017**, *vol. 82*, pp. 34–38.
[69] D. D. Zheng, L. Wang, T. Yang, Y. Zhang, Q. Wang, M. Kurmoo, and M. H. Zeng, *Inorg. Chem.*, **2017**, *vol. 56*, no. 18, pp. 11043–11049.
[70] O. Chiantore and T. Poli, *Atmosphere (Basel).*, **2021**, *vol. 12*, no. 3, pp. 1–19.
[71] M. Panchal, Monik; Nouar, Farid; Serre, Christian; Benzaqui, Marvin; Sene, Saad; Steunou, Nathalie; Gimenez Marqués, "US20210277042A1 - Low temperature process for the synthesis of MOF carboxylate nanoparticles," **2017**.
[72] P. G. M. Mileo, K. H. Cho, J. Park, S. Devautour-Vinot, J.-S. Chang, and G. Maurin, *J. Phys. Chem. C*, **2019**, *vol. 123*, no. 37, pp. 23014–23025.
[73] Y. K. Seo, J. W. Yoon, J. S. Lee, U. H. Lee, Y. K. Hwang, C. H. Jun, P. Horcajada, C. Serre, and J. S. Chang, *Microporous Mesoporous Mater.*, **2012**, *vol. 157*, pp. 137–145.
[74] J. F. Eubank *et al.*, *APL Mater.*, **2014**, *vol. 2*, no. 124112.
[75] Z. Wang, M. Babucci, Y. Zhang, Y. Wen, L. Peng, B. Yang, B. C. Gates, and D. Yang, *ACS Appl. Mater. Interfaces*, **2020**, *vol. 12*, no. 47, pp. 53537–53546.
[76] D. Yang, M. A. Ortuño, V. Bernales, C. J. Cramer, L. Gagliardi, and B. C. Gates, *J. Am. Chem. Soc.*, **2018**, *vol. 140*, no. 10, pp. 3751–3759.
[77] H. Chevreau *et al.*, **2016**, *vol. 18*, no. 22, pp. 4094–4101.
[78] A. García Márquez *et al.*, *Eur. J. Inorg. Chem.*, **2012**, *vol. 100*, no. 32, pp. 5165–5174.
[79] A. Demessence, P. Horcajada, C. Serre, C. Boissière, D. Grosso, C. Sanchez, and G. Férey, *Chem. Commun.*, **2009**, *vol. 101*, no. 46, pp. 7149–7151.
[80] C. Volkringer, H. Leclerc, J. C. Lavalley, T. Loiseau, G. Férey, M. Daturi, and A. Vimont, *J. Phys. Chem. C*, **2012**, *vol. 116*, no. 9, pp. 5710–5719.